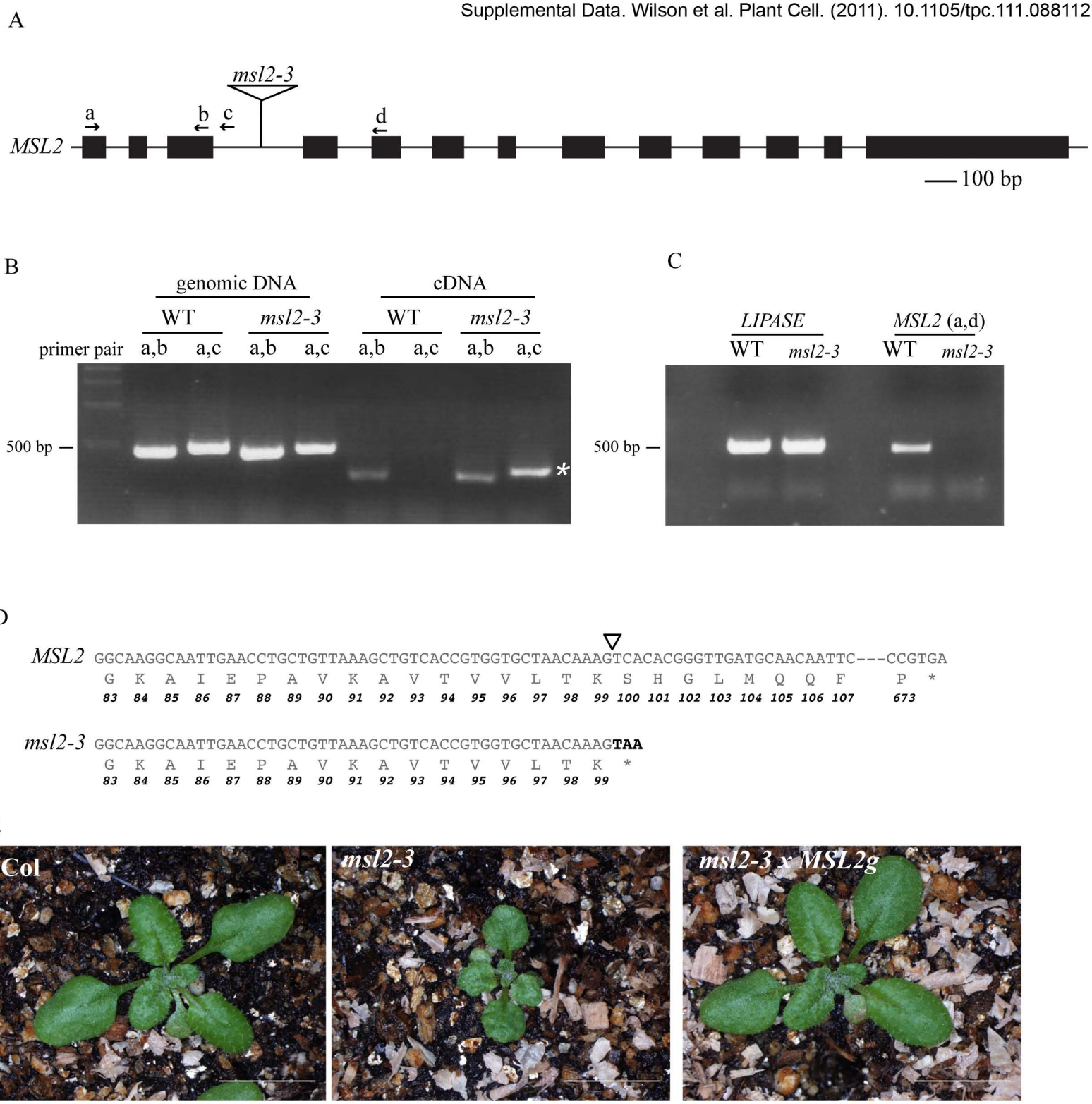

Supplemental Figure 1. Characterization of the *msl2-3* allele.

A) Schematic of the *MSL2* gene. The GK-195D11T-DNA is located 744 bp downstream of the *MSL2* ATG. Boxes and lines indicate exons and introns, respectively. Arrows indicate the location of primers used in panel B. B) RT-PCR on genomic DNA and leaf tissue cDNA derived from wild type and *msl2-3* plants. Amplification of cDNA with primer pair a,c generates a product in the *msl2-3* mutant (asterisk), indicating a defect in splice site selection at the 5' end of the third exon. C) RT-PCR on leaf tissue cDNA derived from wild type and *msl2-3* plants. No transcript spanning the T-DNA insertion site was detected in the *msl2-3* mutant, indicating that the T-DNA is not spliced out. D) Top, wild type cDNA sequence containing the junction between exons 3 and 4 (marked by the arrow). Bottom, *msl2-3* cDNA sequence showing a lack of splicing and instead a stop codon. E). *msl2-3* plant phenotype and complementation by the *MSL2g* transgene, which harbors 5.5 Kb of genomic sequence containing the *MSL2* gene (from 1.5 Kb upstream of the start codon to 350 bp downstream of the stop codon, as described in Haswell and Meyerowitz, 2006).

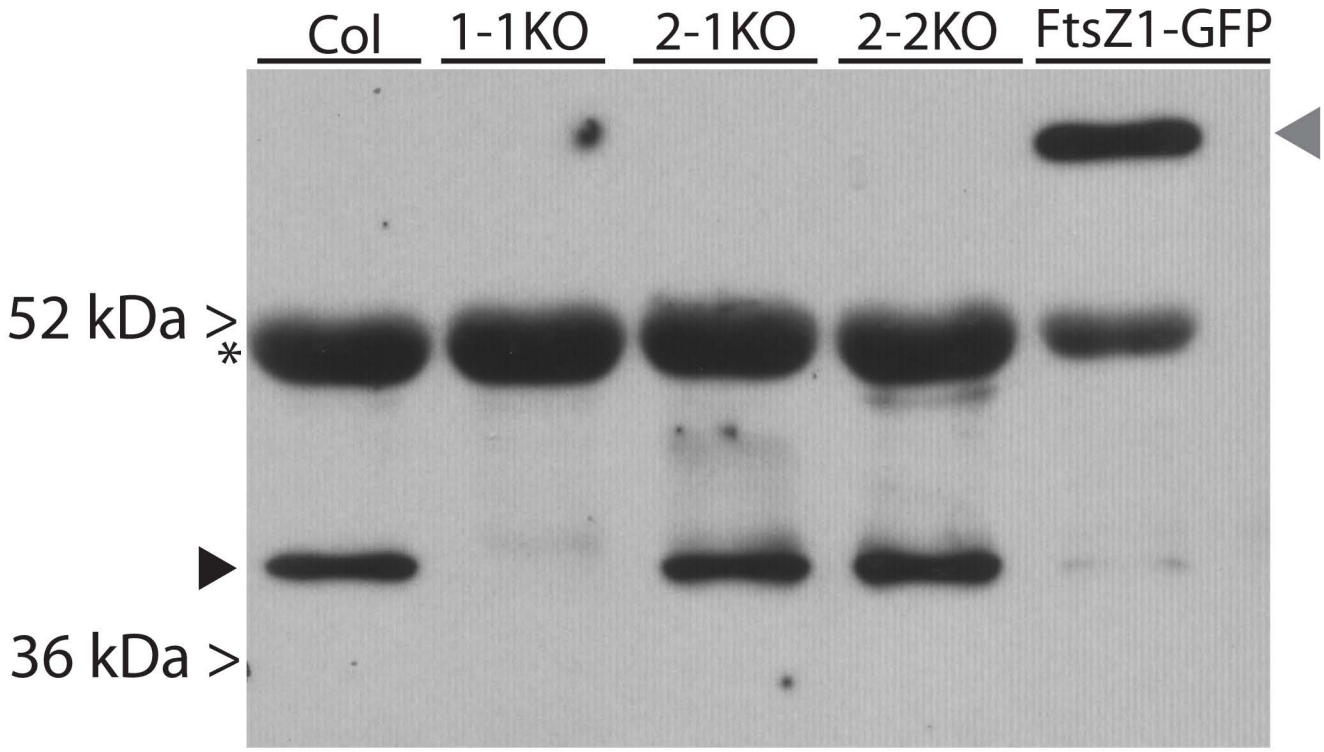

Supplemental Figure 2. An antibody raised against *Bacillus subtilis* FtsZ recognizes *Arabidopsis thaliana* FtsZ1
Immunoblot of *ftsz* knock-out lines 1-1 KO (SALK_073878), 2-1 KO (GABI-Kat 596H04), 2-2 KO (SALK_050397) and a wild type line expressing FtsZ1-GFP. A primary antibody raised against *B. subtilis* FtsZ was used. Bands corresponding to AtFtsZ1 and AtFtsZ1-GFP are indicated with black and grey arrows, respectively. A band at the predicted molecular weight of Rubisco (49 kDa) was used as a loading control and is indicated by an asterisk.

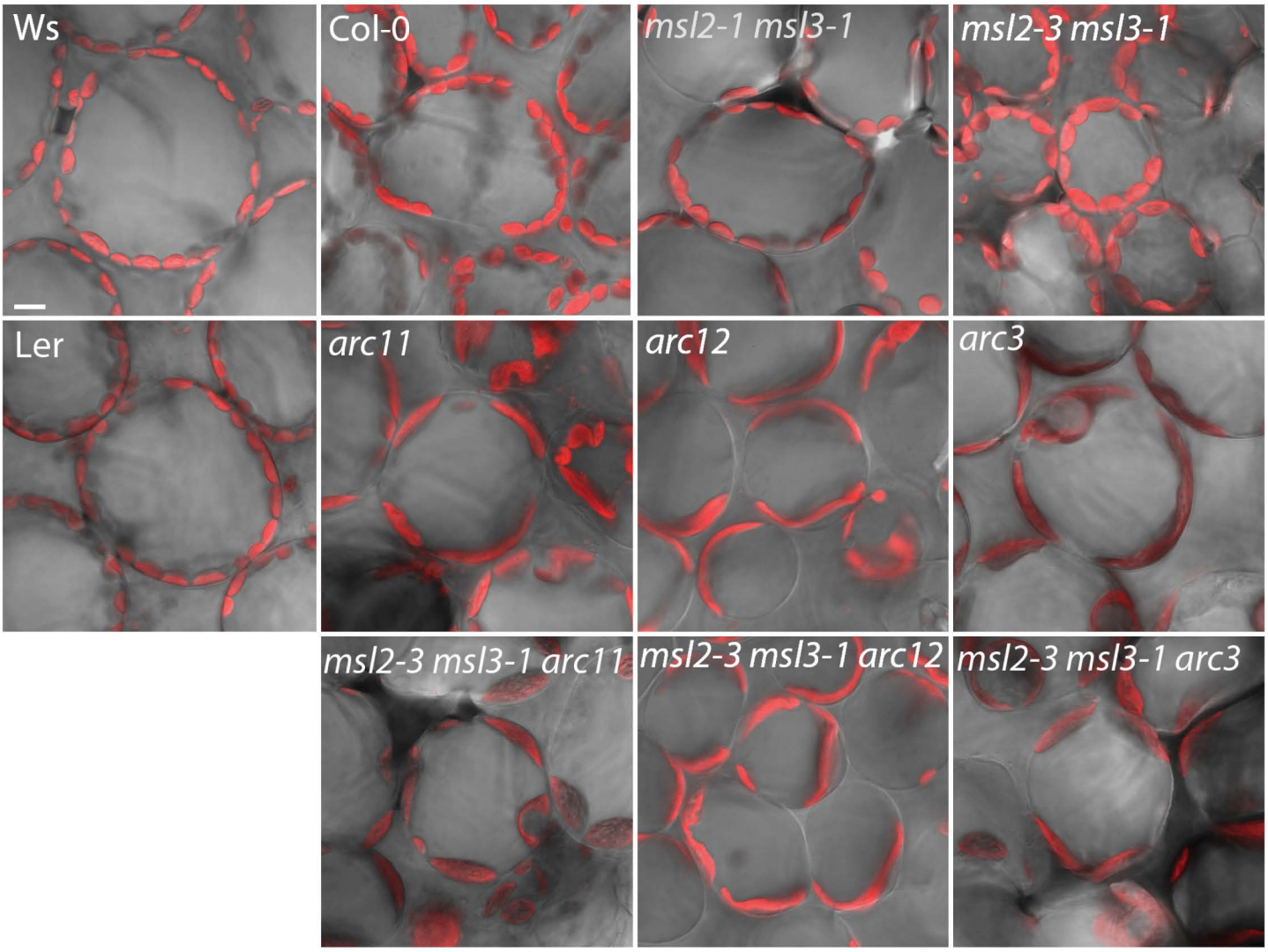

Supplemental Figure 3. Representative images of confocal scans used to determine chloroplast number in single, double and triple *msl* and *arc* mutants

Confocal scans of mesophyll cells show a decrease in the number of chloroplasts per optical section in *msl* and *arc* mutants, as compared to wild type. Chlorophyll fluorescence is shown in red. Scale bar 10 μm; all images were taken at the same magnification.

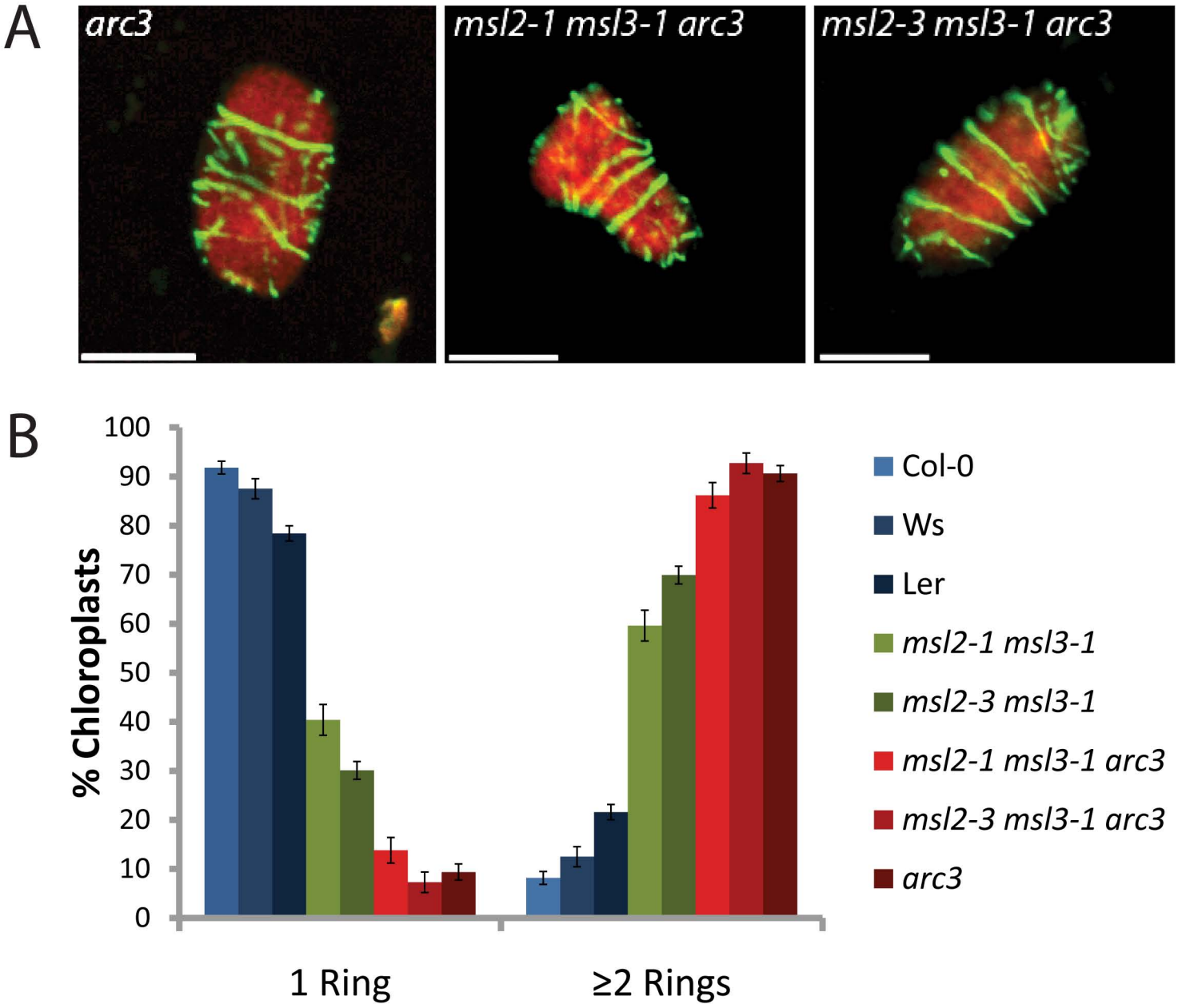

Supplemental Figure 4. *msl2 msl3 arc3* triple mutants are phenotypically indistinguishable from single *arc3* mutants

(A) Immunofluorescent micrographs of Z-ring placement in chloroplasts isolated from rosette leaves of the indicated genotypes. FITC and chlorophyll fluorescence are pseudo-colored in green and red, respectively. Scale bar 10 μm. (B) Quantitative analysis of Z-rings in isolated chloroplasts. The average values from 2 independent experiments ± SE of the means are presented. N ≥ 100 chloroplasts per replicate. No statistically significant difference in the percentage of chloroplasts containing 2 or more rings was observed in *msl2 msl3 arc3* triple mutants compared to *arc3* single mutants (Student's T-test, $p > 0.2$).

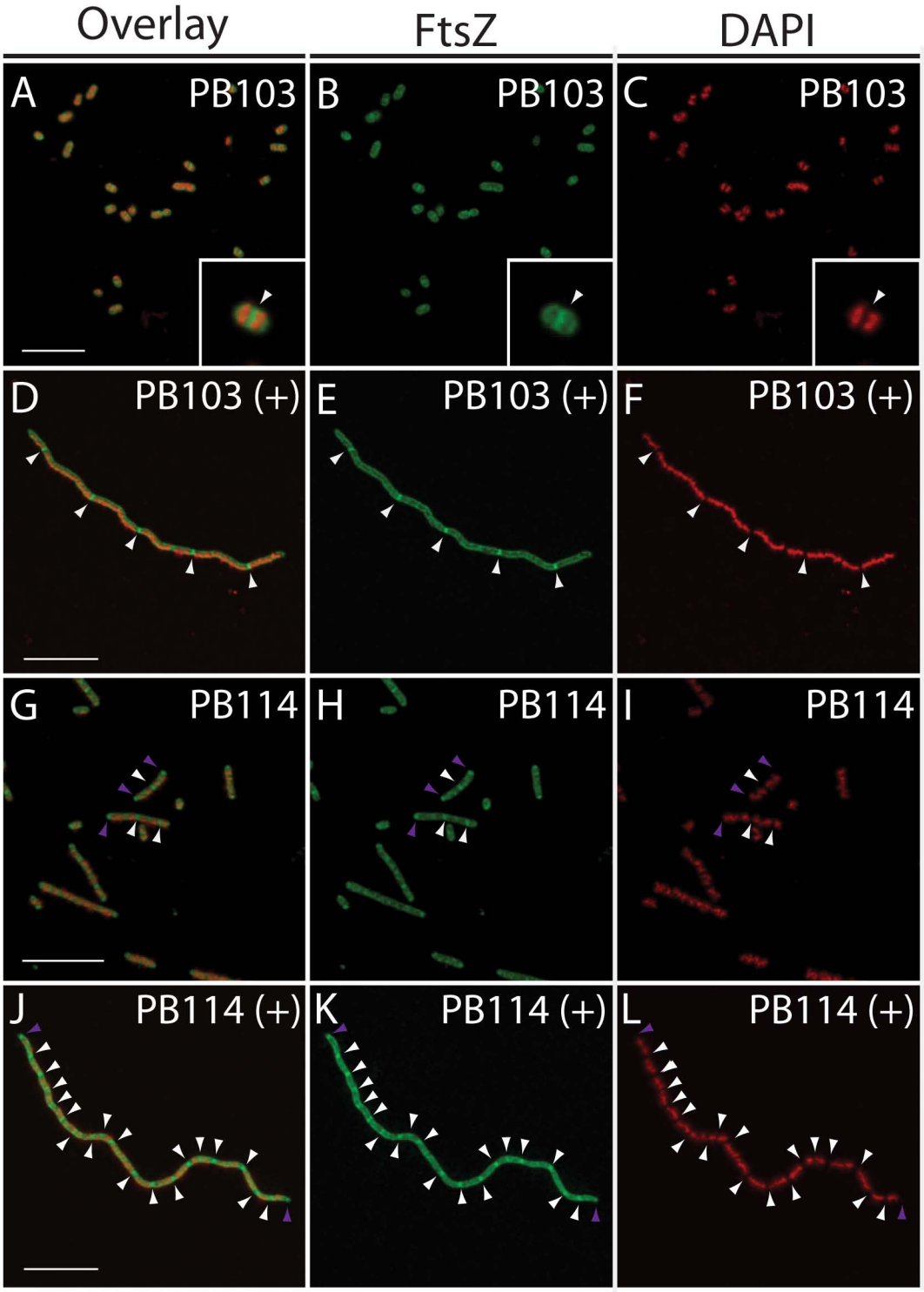

Supplemental Figure 5. Z-ring placement in the Δ*minB* strain of *E. coli*

Immunofluorescent micrographs of FtsZ (pseudo-colored green) and DAPI staining of nucleoids (pseudo-colored red) in PB114 *(ΔminB*) and PB103 (wild type) cells. Cells were grown with (D-F, J-L) or without (A-C, G-I) 10 mM cephalexin for 1 hr prior to fixing. White arrowheads indicate individual Z-rings. Purple arrowheads indicate polar Z-rings (G-L). Scale bar is 10 μm.

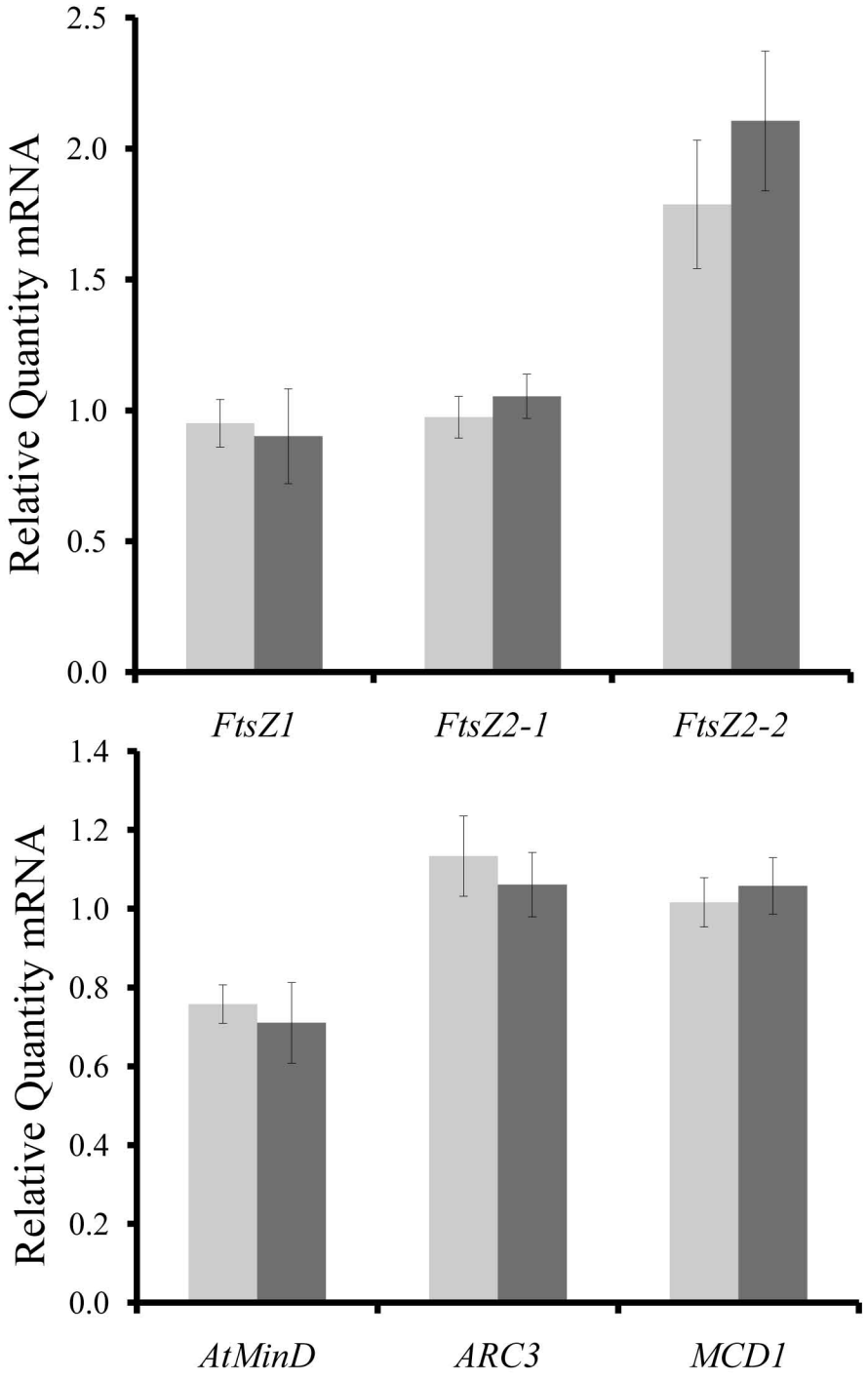

Supplemental Figure 6. Transcript levels of genes involved in chloroplast division are not altered in *msl2 msl3* mutants.

Quantitative RT-PCR analysis of chloroplast division gene expression in wild type Col-0 (light bars) and *msl2-3 msl3-1* (dark bars) plants, normalized to *ACTIN*. The average mean of three biological replicates (each with three technical replicates) is presented, and error bars indicate the standard deviation of the means. No significant changes in transcript levels between the two samples were observed (student's t-test, $p > 0.4$).

Table S1. Oligos used in Genotyping and qRT-PCR	
Name	**Sequence**
10490.F4	TGAAGACGTCTCATCACGAAG
2.3'	TTACATCATGACTAGAGACAGGTAAGCTA
58200.F8	GCCGATACATGCTGATTGAG
3.3'	TTTCTCCGTTTCTGTTTGTTACTTTCTAC
JL-202	CATTTTATAATAACGCTGCGGACATCTAC
MSL2BF.Sal	ACGCGTCGACATGGCCCTTTATGGTACATTG
msl2.R4	GAAGAGCAACAGCTGGAACC
LB.GABI	CCCATTTGGACGTGAATGTAGACAC
MSL2(a)	CACCATGACTTCATATGTTCAACCTCTGTTAC
MSL2(b)	ACTTTGTTAGCACCACGGTGACAG
MSL2(c)	GGTCATTCTGCATGTGATGATAGGAAACAAG
MSL2(d)	AACATGGTACGTACCACTCTTCTTCC
arc3.DCAPs.F2	TCCAAGGCACATGGAGAGAAGA
arc3.DCAPS.R6	CCATCGATCACCTTTGTGCAAATGATA
arc11.DCAPS.F	GGGATTGGCGTTTGAGCATG
arc11.DCAPS.R	TCAGAGCTTGAACTCAGCAACA
arc12DCAPS.F	GGGTTTCTTTGACAGGTTAACCATG
arc12DCAPS.R	CGTCTTGGTACTCTGGTTTCAC
FtsZ1.QPCR.F	CCGGATGATTTCAAGCGGTTTACAG
FtsZ1.QPCR.R	GCCAAGCCCAACGAGTTAAAAGTTC
FtsZ2-1.QPCR.F	CTGGCGGAAGTGACTTGACATTG
FtsZ2-1.QPCR.R	CCGCTGAGGGCTGGATCTAC
FtsZ2-2.QPCR.F	CCTCGTTGATCCAACAGCGAATC
FtsZ2-2.QPCR.R	CCGCTTGTGTCGCCTGAAG
MinD.QPCR.F	GGAATGGCTTGTGGATGCGTTG
MInD.QPCR.R	CTGCTTCATTCGCCGGAGTAATG
ARC3.QPCR.F	CTATCCGCTCGAGCATCGTCTATG
ARC3.QPCR.R	GAAGGCCCCTTGGCATCTTC
MCD1.QPCR.F	CGCACATCTCTACCGTTGAGCTTC
MCD1.QPCR.R	GCCAAGCTGAGGTCTGGTGATAG

Supplemental Table 1. Oligos used in genotyping and quantitative RT-PCR